Solid Freeform Fabrication 2021: Proceedings of the 32nd Annual International
Solid Freeform Fabrication Symposium – An Additive Manufacturing Conference
Reviewed Paper

Utilizing Additive Manufacturing in Thermoacoustic Refrigeration-based Atmospheric Water Generation

Zaid Almusaied and Bahram Asiabanpour
Ingram School of Engineering, Texas State University, San Marcos TX 78666

Abstract

Atmospheric water generators are devices that generate water by condensation. The water vapor in the air is cooled, by a refrigeration system, below the dew point and thus forces a phase transfer from gaseous to liquid. Thermoacoustic refrigeration (TAR) was used as the refrigeration technology. The TAR is an innovative clean technology that utilizes an acoustic wave passing through a gas to create a temperature gradient in a specially designed porous material. The main components of such a system are resonator tube, stack, acoustic driver, gas, and heat exchangers. An additive manufacturing process was utilized to develop different configurations and interchangeable components of the TAR system. The lowest temperature on the cold side of the stack was achieved by the stack manufactured with spiral design, spacing of 0.53 mm, 4cm length, and 1cm stack position in the resonator tube. The minimum temperature achieved with this prototype was around 46˚F at a room temperature of 72˚F, relative humidity of 59%, and dew point of 57˚ F.

Introduction

Water scarcity and the decrease in its quality are immense threats to nations' existence and prosperity. 71% of the globe is covered by water. Yet only 1% of that water is potable water [1]. The projection for 2025 shows a water shortage crisis affecting 1.8 billion people [2]. The increase in water demand can be attributed to the continuous growth in population, agriculture, industry, changes in living conditions, and diet [3]. The problems associated with potable water needs are not restricted to developing countries. Still, they can also impact the developed ones too, as the case of water contamination in Flint, Michigan, indicates. The water in the atmosphere can be used to solve water scarcity. The projection of the water in the atmosphere is 3000 cubic miles [1]. The use of atmospheric water is done by devices called Atmospheric Water Generators (AWG). Atmospheric water generators are devices that generate water by condensation. The water vapor in the air is cooled by a refrigeration system below the dew point, forcing a phase transfer from gaseous to liquid. The AWG's main components are the cooling system, the water condensation-collection surfaces, and the water purification system. The components of the AWG are shown in Figure 1.

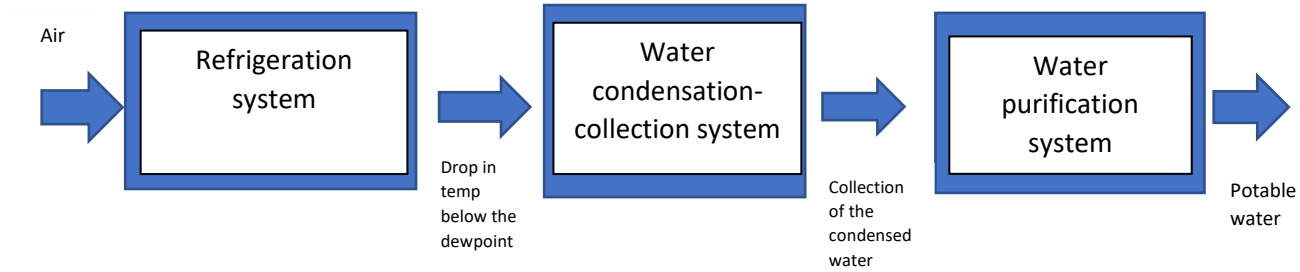

Figure 1: AWG main component and processes.

In general, for AWG's refrigeration system, the current products in the market use vapor-compression refrigeration technology (VCR). The use of refrigerant gas by VCR technology brings environmental risks of ozone depletion and/or global warming [4]. On the other hand, thermoacoustic refrigeration (TAR) can be used as an alternative-eco-friendly for the VCR refrigeration system. The TAR is an

innovative clean technology that utilizes an acoustic wave passing through a gas to create a temperature gradient in a specially designed porous material.

Thermoacoustic Refrigeration

A sound wave passing through a gas is a mechanical longitudinal wave. The passage of the sound wave will generate fluctuations in pressure, displacement, and temperature. The oscillations interact with the solid boundaries of the system in various ways. A thermoacoustic effect will result from this interaction [5]. The thermal effects are not sensed with ordinary speech sound levels. The variation in temperature will barely be a ten-thousandth of a degree centigrade [6], but with high-intensity sound in pressurized resonant craters crafted into multiple types of heat exchangers, the thermoacoustic effects can be then exploiting to make a good heat engine or refrigerator [7]. The implementation of the thermoacoustic phenomenon to create a cooling system started to gain rapid attention during the last couple of decades. This promising technology has many advantages when compared to conventional cooling systems. The most prominent advantage is its use of gases that carry no hazardous implication on the environment instead of regular refrigerants. TAR can use air or inert gases such as helium [8]. The system also uses loudspeakers, which perform a close function of the compressor, the source of the provided work, in the conventional cooling systems. This is considered to be another advantage since they are more durable and simpler than the traditional compressors [9]. The thermoacoustic systems can be categorized into thermoacoustic engines and thermoacoustic refrigerators. The thermoacoustic engines take the heat from the high-temperature side, transform it into acoustic energy, and deposit the unused heat into the cold side [10]. The thermoacoustic refrigerators are heat pumps that move the heat, as external work is applied, from one side to the other and create a temperature gradient, as shown in Figure 2 [8] [11]. Both thermoacoustic engine and refrigerator can be divided into standing wave or traveling wave (pulse tube) devices, based on the type of acoustic wave used in the system [9].

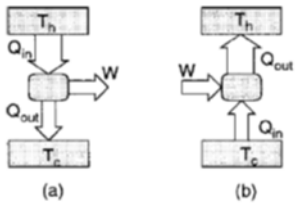

Figure 2: The basic action of (a) heat engine, (b) heat pump [11].

Basic TAR Components

The basic thermoacoustic refrigerator consists of the following parts: resonator tube, stack, acoustic driver, gas, and heat exchangers [12]. The parts of the simple TAR are shown in Figure 3.

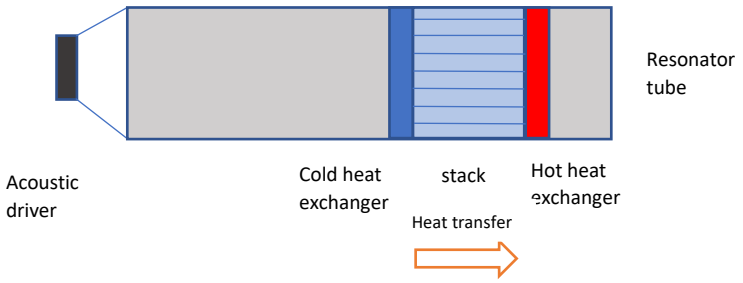

Figure 3: Thermoacoustic refrigerator. The system consists of an acoustic driver, stack, heat exchangers, resonator tube, and gas.

The temperature gradient along the stack can be created without the existence of the heat exchangers [13]. The change in the gas's temperature can be traced to its adiabatic compression and expansion due to the passing of the acoustic pressure and to the heat transfer with the stack [5]. The simplification of this idea can be seen in the next figure.

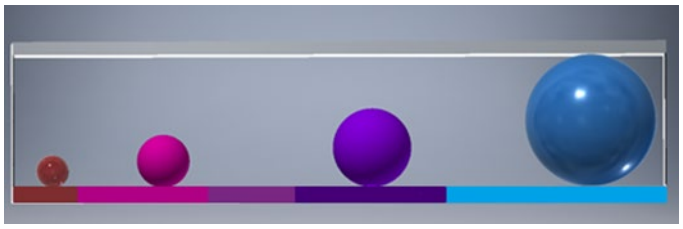

Figure 4: The interaction between a parcel of gas and the stack's wall. The acoustic wave causes the parcel to go under compression and expansion and thus, creating an oscillation in its temperature.

The parcel of gas will dump its heat to the stack when its temperature is higher than the adjacent stack's wall. This rise in the temperature of the parcel of gas is a result of the adiabatic compression initiated by the standing sound wave. The next step in the cycle will occur as the parcel will undergo an adiabatic expansion due to the rarefaction of the sound wave, which will lead to an increase in its volume and dropping in its temperature. The parcel's temperature in this stage will be less than the adjacent stack's wall, and thus, the heat will transfer from the stack to the parcel. The overall result of this process is a creation of a temperature gradient along the stack wall. The design of a TAR that can achieve a powerful refrigeration effect requires an identification of the variables related to its main components and the effect of each variable on the temperature gradients and on each other. Some of the characteristics and design variables for each component of the TAR are listed below:

The Gas: The used gas in the TAR system should have a high thermal penetration depth $\delta_k$and low viscous penetration depth δ_v [13] [14]. The thermal penetration depth is proportional to the square root of the thermal conductivity of the gas, and thus it reflects the gas's capacity to transfer the heat through its boundary [13] [15].

$$\delta_k = \sqrt[2]{\frac{k}{\rho c_p \pi f}} \qquad \text{---------(3)}$$

Where k,ρ, c_p, and f are, respectively, the gas's thermal conductivity, density, specific heat, and the frequency of the sound wave. The viscous penetration depth of the gas needs to be small to minimize its fractional losses.

$$\delta_v = \sqrt[2]{\frac{\mu}{\rho \pi f}} \qquad \text{----------(4)}$$

Where μ, ρ, and f are, respectively, the gas's viscosity, density, and the frequency of the sound wave. The Prandtl number (σ) is the ratio of the square of the viscous penetration depth to the square of the thermal penetration depth. This number needs to be minimized. The ratio of the acoustic wave amplitude to the gas mean pressure, which is denoted as the drive ratio, needs to be reduced to avoid the nonlinearity of the acoustic wave [13].

$$D = \frac{P_o}{P_m} \text{----------(5)}$$

Where D, P_o, and P_m are, respectively, the drive ratio, the acoustic wave amplitude, and the gas mean pressure.

The selected gas needs to have a high ratio of the isobaric heat capacity to the isochoric heat capacity to increase the temperature gradient along the stack wall [13][14].

***The Acoustic Driver*:** The acoustic driver is a transducer that converts electricity into acoustic waves; thus, it is the provider of the required work in the TAR system to accomplish a heat transfer from the cold side to the hot side of the stack. Part of the acoustic power provided by the acoustic driver will be dissipated in the resonator tube and the heat exchangers [14]. The power density of the TAR system will increase as the amplitude of the acoustic wave increases. This increase in the amplitude of the acoustic wave is still governed by the gas mean pressure to avoid nonlinearity.

$\dot{w}_t = \dot{w}_s + \dot{w}_{res} + \dot{w}_{chx} + \dot{w}_{hhx}$-------(6) [14]

Where $\dot{w}_t$, $\dot{w}_s$, $\dot{w}_{res}$, $\dot{w}_{chx}$, and $\dot{w}_{hhx}$ are respectively: the total acoustic power, the dissipated acoustic power in the resonator, the dissipated acoustic power in the cold-side heat exchanger, and the dissipated acoustic power in the hot-side heat exchanger [14].

Thus, the Coefficient of Performance (COP) for the TAR system can be obtained using the following equation:

$\text{COP} = \frac{\dot{Q}_c}{\dot{w}_t}$ ----------(7) [14]

Where $\dot{Q}_c$ is the cooling power of the TAR system. The frequency of the acoustic wave is associated with the resonator length, the thermal penetration depth of the gas, and the design of the stack.

***The Resonator*:** The resonator length is inversely proportional to the frequency of the acoustic wave.

$v = \lambda * f$--------(8)

Where $v, \lambda, and\ f$ are respectively the speed, the wavelength, and frequency of the acoustic wave in the gas.

The TAR resonator-tube length can be either a quarter of the wavelength or half of the wavelength for the first harmonic based on open-closed ends or open-open ends.

The material of the resonator needs to achieve the reflectivity of the acoustic wave and to have low thermal conductivity. The type of gas to be used in the system and its mean pressure will have a strong influence on the design of the resonator. The high mean pressure of the gas will require a resonator tube design to withstand the pressure and to avoid any leakage of the gas. The diameter of the resonator is determined by the stack dimensions and geometry.

***The Stack*:** The stack can be defined as a porous material that converts the oscillation of the acoustic pressure into a temperature gradient. The stack's material needs to have a low thermal conductivity to maintain the building of the thermal gradient across it. Another important property of its material is to have a higher heat capacity than the used gas to minimize the effect of the gas's temperature oscillation and thus build a steady temperature gradient across it [10]. The stack porous geometry needs to achieve a thermal efficiency of the heat transfer between the gas and the stack and reduce the viscous losses within the stack [13]. The thermal and viscous penetration depth of the gas is used in the design of the stack to achieve the previous goal. The spacing between the walls of the stack needs to be between two to four

times the lengths of the thermal penetration depth [16]. The normalized stack's position (X_n) and length (L_{sn}) be calculated through the following equations [14]:

$$Q_{cn} = \frac{\delta_{kn} D^2 Sin2x_n}{8\gamma(1+\sigma)\Lambda} \left[\frac{\Delta T_{mn} \tan X_n}{(\gamma-1)BL_{sn}} \frac{1+\sqrt{\sigma}+\sigma}{1+\sqrt{\sigma}} - 1 + \sqrt{\sigma} - \sqrt{\sigma\delta_{kn}}\right] \text{-----(9)}$$

$$W_n = \frac{\delta_{kn} L_{sn} D^2}{4\gamma} (\gamma-1) B cos^2 x_n \left[\frac{\Delta T_{mn} \tan X_n}{BL_{sn}(\gamma-1)(1+\sqrt{\sigma})\Lambda} - 1\right] - \frac{\delta_{kn} L_{sn} D^2}{4\gamma} \frac{\sqrt{\sigma}\ sin^2 x_n}{B\Lambda} \text{------(10)}$$

$$\Lambda = 1 - \sqrt{\sigma}\ \delta_{kn} + 0.5\ \delta_{kn}^2 \text{----(11)}$$

WhereQ_{cn}, δ_{kn}, ΔT_{mn}, and W_n are respectively the normalized cooling power, thermal penetration depth, temperature difference, and acoustic power. The normalization of the parameters of the equation is achieved by using the following equations in table 1. Λ is an intermediate parameter, D is the driving ratio, σ is the Prandtl number, and γ is the ratio of the specific heats.

The blockage ratio of the stock is denoted as B and is calculated by the following equation:

$$B = \frac{y_\circ}{y_\circ+1} \text{-----(12)}$$

Where $y_\circ$ is half the spacing between the layers of the stack.

Table 1. The normalization formulas [17] [14].

$Q_{cn} = \frac{Q_c}{P_m a A}$, where a and A are the sound velocity and the cross-section of the stack	L_{sn}=KL_s, K and L_s are the wavenumber and the stack's length
$W_n = \frac{W}{P_m a A}$, where a and A are the sound velocity and the cross-section of the stack	X_n= KX, K, and X are the wavenumber and the stack's position
$\Delta T_{mn} = \frac{\Delta T_m}{T_m}$, where ΔT_m and T_m are the temperature difference and the average temperature.	$\delta_{kn} = \frac{\delta_k}{y_\circ}$, δ_k and $y_\circ$ are the thermal penetration of the gas and the stack's half spacing.

The stack coefficient of performance can be expressed as

$$\text{COP} = \frac{Q_{cn}}{W_n} \text{-----(13)}$$ [14].

***The Heat Exchangers*:** The heat exchangers can be used to achieve heat movement between the TAR system and the outside. That being said, the TAR system can be built without the heat exchangers, and the temperature gradient will still be generated across the stack. Thus, the heat exchangers are important to make the cooling power, generated by the TAR, of a user to the user when they are connected to the stack sides and to the outside thermal loads. The two ends of the stack will be attached to the hot and the cold heat exchangers. The length of a heat exchanger is associated with the distance that the gas can transfer the heat through it [14]. The porosity of a heat exchanger should match the porosity of the neighboring stack to ensure a continuous volume velocity of the gas [10].

In this research, a thermoacoustic refrigerator is designed to achieve a drop in temperature below the dew point. This will ensure a capability to condense the water vapor and generate water. Multiple stacks with different dimensions, locations in the resonator, and fabrication methods were explored to achieve the

aforementioned goal. Additive manufacturing was utilized to fabricate different components of the system, including the stack.

Fabrication of the TAR and experiment settings

The working gas for the TAR system used in this research utilized air under atmospheric pressure.

- **The resonator** was designed and implemented to achieve the quarter wavelength criteria. The resonator had one end attached to the speaker, and the other was closed with a plug. The plug was designed with AutoCAD inventor and printed with an FDM printer, as demonstrated in Figure (5). The plug insured a passage for the temperature sensor wires. The material of the resonator was acrylic with a diameter of 4.125cm and a wall thickness of 0.32 cm. The length of the resonator was 23cm. Thus, the theoretical resonance frequency was calculated using equation eight to be 377 HZ, with the speed of sound in the gas equal to 347 m/s. The actual resonance frequency was obtained by manually tuning the system and observing the signal through a condenser microphone and an oscilloscope. Thus, the operational resonance frequency was found empirically to be 341 HZ.

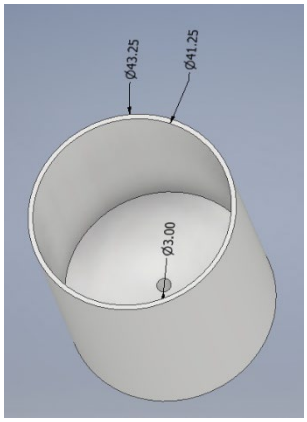

Figure 5: CAD design of the resonator plug. The plug contained a hole in the middle to have the sensors wires passing through; additionally, silicone sealant was used around the wires to ensure tight sealing.

- **The acoustic driver**, an on-shelf 400 watts loudspeaker used in the TAR system, was fed with an acoustic signal generated by a function generator through an audio amplifier. The acoustic signal used in the tests was sinusoidal, and it was measured through the use of a small condenser microphone connected to an oscilloscope.
- **The temperature measurement**: the temperature gradient on the two ends of the stack was measured through the use of two k-type thermocouples.
- **The stack**: Multiple stacks with different dimensions were designed and tested. The stacks were made either using additive manufacturing or using an in-lab-designed spiral technique. Two 3D printers were explored to make the stacks. The first printer was based on Fused deposition modeling (FDM) technology, while the second was based on Stereolithography (SLA) 3D printing. The 3D printed stacks were designed with AutoCAD Inventor software. The FDM printer material was Acrylonitrile butadiene styrene (ABS). The designs for the 3D printed stacks included parallel plates, circular holes, and honeycomb, as demonstrated by Figure 6. The thermal penetration depth was calculated using equation three, and it was found to be around 0.14mm.

Thus, the goal for the spacing in the stack was supposed to be between two to four of the thermal penetration depths. The spiral design was implemented with a plastic sheet and fishing lines glued to the sheets to control the spacing between the layers, as shown in Figure 7. The fishing lines' diameters were controlling the spacing between the stacks. Two fishing lines were explored, the first was with a diameter of 0.53mm, and the second was 0.33mm. The spacing between the glued fishing lines was 0.5cm. The apparatus used to make the spiral sheet stack is shown in Figure 8. All fabricated stacks had a length of 4cm or 5cm.

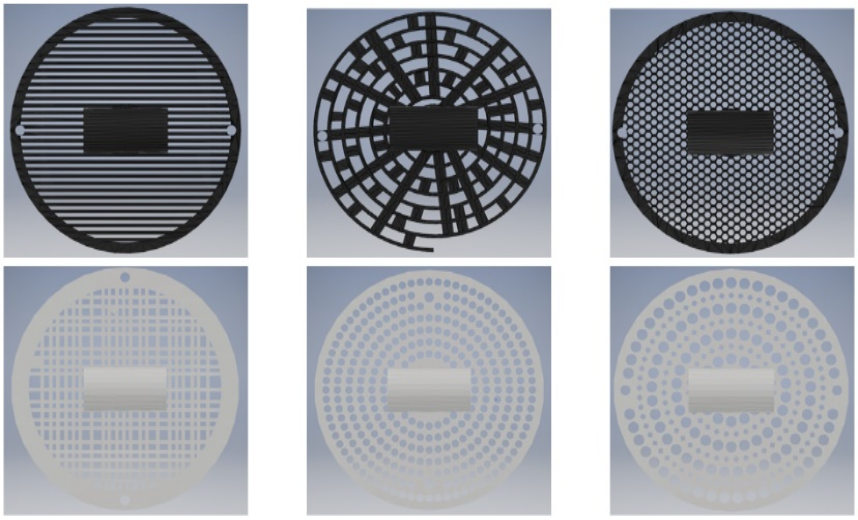

Figure 6: The CAD designs for multiple stacks. The designs included parallel plates, circular holes, and honeycomb.

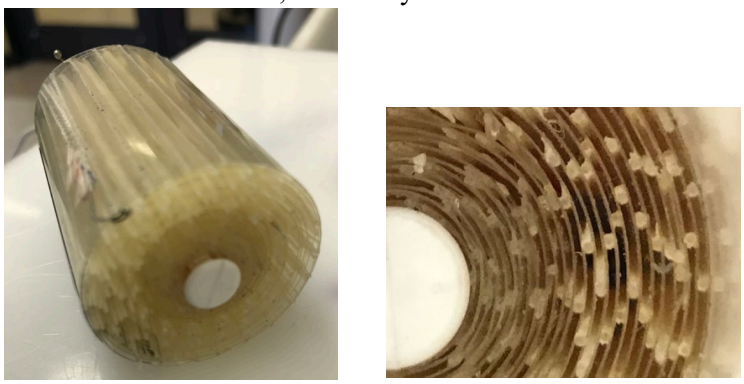

Figure 7: A. The spiral stack made using plastic sheets and fishing lines. B. The cross-section of the spiral stack

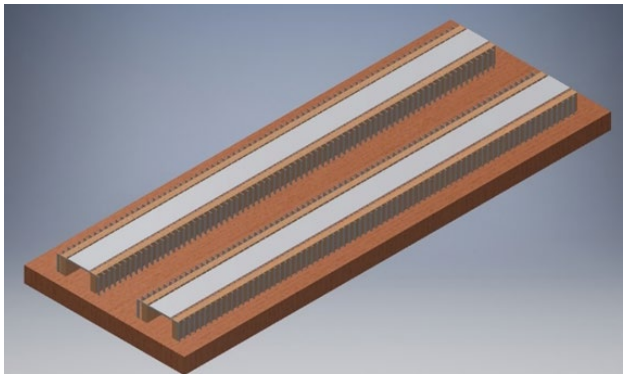

Figure 8: A simple loom to fabricate a spiral design stack.

- The ambient temperature and relative humidity were obtained using a handheld meter. Different stacks with various geometry, length, material, position in the resonator, and inner spacing varied during the runs. Each run lasted for three minutes, and the system was cooled down in between the runs until the temperature between the stack's sides was the same. The experiment components are illustrated in Figure 9.

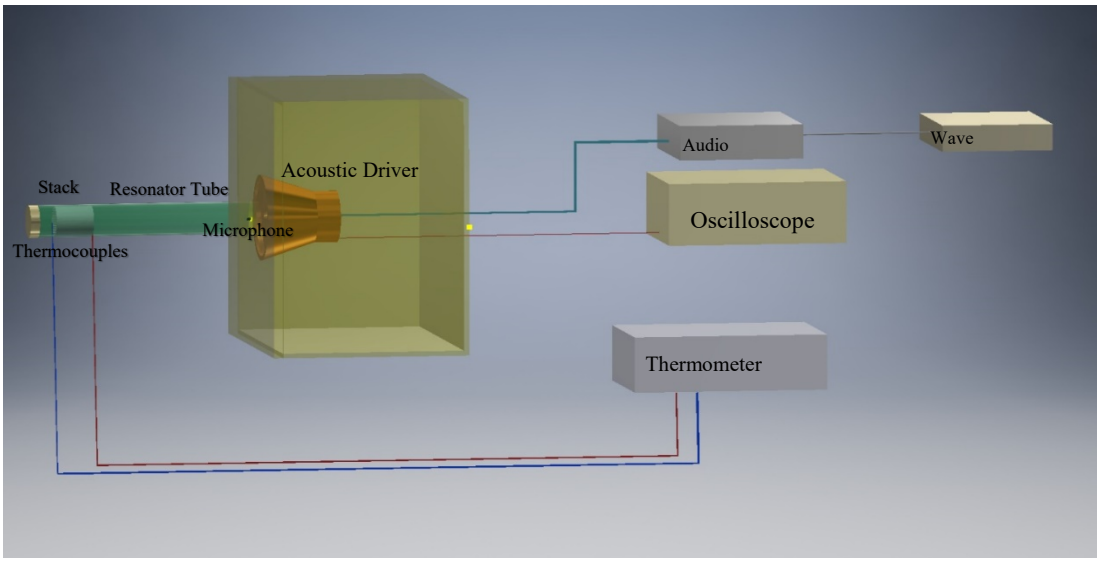

Figure 9. Schematic of the experiment components.

Result and discussion

The 3D printed stacks were only successful when manufacturing the parallel plate stacks with 1mm spacing and 4cm length, shown in Figure 10. The other designs with smaller spacing suffered from defects, shown in Figure 11, where the inner walls were damaged. The stacks made with SLA were also unusable due to the residue of resin in the spacing; this caused a blockage inside them.

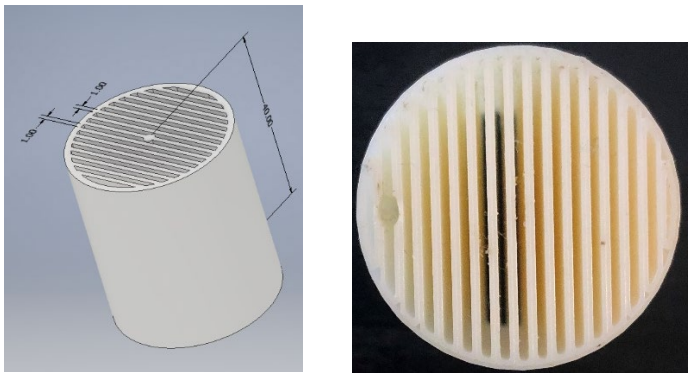

Figure 10. A. Stack CAD design with parallel plates having 1mm spacing between them. B. The parallel plates stack printed by FDM printer with 1mm spacing between the plates

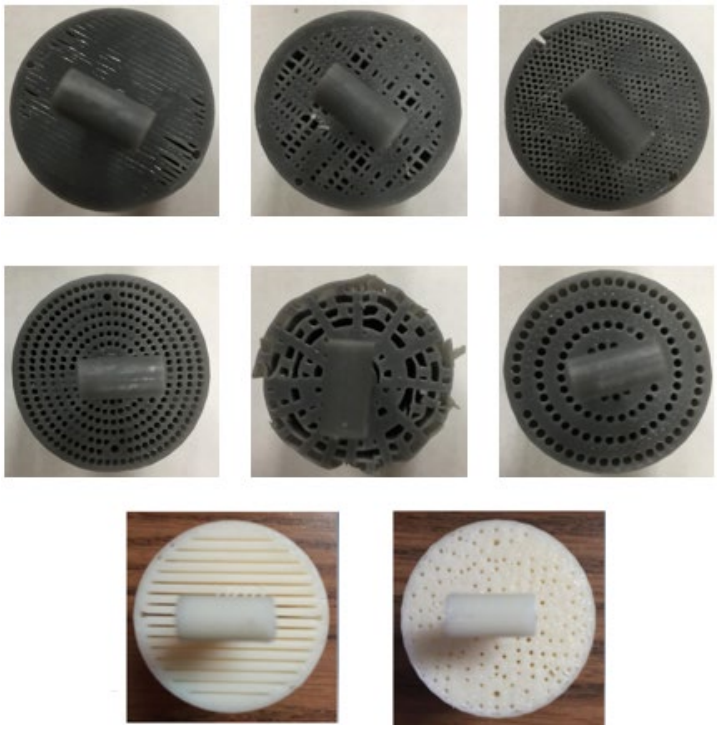

Figure 11: The defective 3D printed stacks.

The overall manufactured TAR is illustrated in figure eight, and the result of the experiment is shown in the next table

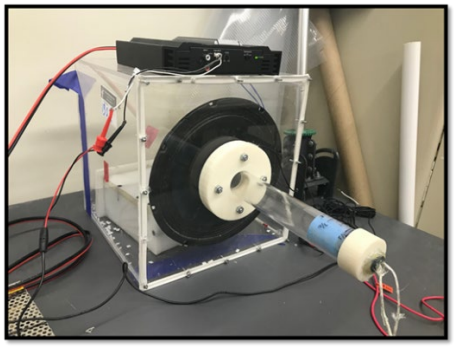

Figure 12. The constructed TAR system.

The lowest temperature on the cold side of the stack was achieved by the stack manufactured with spiral design, spacing of 0.53 mm, 4cm length, and 1cm stack position in the resonator tube. Thus, the aforementioned stack was capable of achieving the biggest difference between the hot and cold sides and the biggest drop in temperature below the dew point, as illustrated by both Table 2 and Figure 13. The minimum temperature achieved with this prototype was around 46˚F at a room temperature of 72˚F, relative humidity of 59%, and dew point of 57˚F.

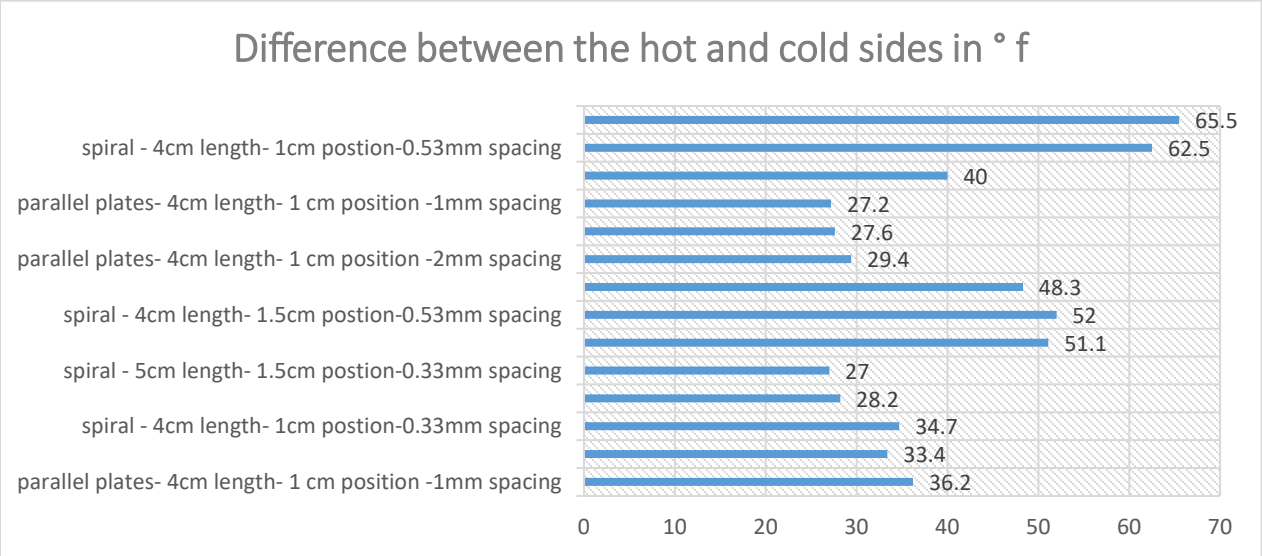

Figure 13. The fabricated stacks and their differences between the hot and cold sides.

Table 2. The experiment results for all the manufactured stacks

RTºf±0.05	RH% ±0.05	Dew point	Stack type and material	Stack manufacturing method	Stack length cm	Stack spacing mm	Stack position cm	Cold-ide temp ºF±0.05	Hot-side temp ºF±0.05	Difference between the hot and cold sides in ° F	Difference between the cold sides and the dewpoint in ° f
77	55.4	59.8°	parallel plates ABS	FDM	4	1	1	69.3	105.5	36.2	9.5
78.5	50.5	58.6°	parallel plates ABS	FDM	4	1	1	66.6	100	33.4	8
78.4	50.2	58.3°	spiral plastic sheet	loom	4	0.33	1	66	100.7	34.7	7.7
80	45	56.7°	spiral plastic sheet	loom	5	0.33	1	67.8	96	28.2	11.1
81	46	58.2°	spiral plastic sheet	loom	5	0.33	1.5	70	97	27	11.8
83	43	58.2°	spiral plastic sheet	loom	4	0.53	1.5	63.6	114.7	51.1	5.4
73.3	58	57.6°	spiral plastic sheet	loom	4	0.53	1.5	53	105	52	-4.6
72.8	57.8	57.1°	spiral plastic sheet	loom	4	0.53	1	54.7	103	48.3	-2.4
73.4	57.4	57.4°	parallel plates ABS	FDM	4	1	2	65	94.4	29.4	7.6
72	58	56.4°	parallel plates ABS	FDM	4	1	1.5	64.4	92	27.6	8
73	57	56.9	parallel plates ABS	FDM	4	1	1	63.8	91	27.2	6.9
73	57	56.9	spiral plastic sheet	loom	5	0.53	2	57	97	40	0.1
73.8	55.8	57	spiral plastic sheet	loom	4	0.53	1	51.5	114	62.5	-5.5
72	59.3	57	spiral plastic sheet	loom	4	0.53	1	46.5	112	65.5	-10.5

Conclusion

In this research, a TAR was designed and implemented to create a drop in temperature below the dew point. Multiple stacks with different spacing, lengths, positions in the resonator tube were tested. Additive manufacturing was explored to make the heart of the TAR (the stack). The FDM and SLA were tested to make a stack with different designs. Only the FDM printed stack with parallel plates, and 1mm spacing was printable with clear spacing. The other manufacturing method used to fabricate the stack was a simple loom. The spacing controlled for the spiral designs manufactured with the loom was achieved using fishing lines with different diameters. The difference between the hot-side and the cold-side of the stacks was measured, and it was significant for all of them. Yet only one spiral with 0.53 spacing was capable of achieving the desired drop below the dewpoint. The next step to achieve the goal of harvesting

water is adding heat exchangers to the stack where the drop in temperature can be utilized to generate water.

References

1. Howard Perlman, U. (2017). How much water is there on Earth. *USGS Water Science School*. Water.usgs.gov. Retrieved 25 March 2021, from https://water.usgs.gov/edu/earthhowmuch.html
2. Stronger Cooperation on Transboundary Aquifers, Basins Key to Resolving Conflict over Finite Resource, Deputy Secretary-General Tells Water Diplomacy Panel | Meetings Coverage and Press Releases. (2021). Retrieved 4 May 2021, from https://www.un.org/press/en/2018/dsgsm1210.doc.htm
3. Almusaied, Z., & Asiabanpour, B. (2017). Atmospheric Water Generation: Technologies and Influential Factors. IIE Annual Conference. Proceedings, 1448.
4. Publications, C. (2019). Refrigerants and their environmental impact. Retrieved from http://crown.co.za/featured/5457-refrigerants-and-their-environmental-impact.
5. Swift, G. W. (1995). Thermoacoustic engines and refrigerators. (cover story). Physics Today, 48(7), 22. https://doi.org/10.1063/1.881466
6. Garrett, S. L. (1), & Backhaus, S. (n.d.). The power of sound. American Scientist, 88(6), 516–525. https://doi.org/10.1511/2000.6.516
7. Swift, G. W. (2000). Streaming in thermoacoustic engines and refrigerators. AIP Conference Proceedings, 524(1), 105. Retrieved from http://libproxy.txstate.edu/login?url=http://search.ebscohost.com/login.aspx?direct=true&db=edb&AN=5665320&site=eds-live&scope=site
8. RAUT, A. S., & WANKHEDE, U. S. (2017). Review of Investigations in Eco-Friendly Thermoacoustic Refrigeration System. Thermal Science, 21(3), 1335–1347. https://doi.org/10.2298/TSCI150626186R
9. Thermoacoustic Refrigerators - Thermal Systems. (2019). Retrieved from http://me1065.wikidot.com/thermoacoustic-refrigerators.
10. Tijani, M. (2001). Loudspeaker-driven thermo-acoustic refrigeration. Technische Universiteit Eindhoven.
11. Russell, D. A. (1), & Weibull, P. (1,2). (n.d.). Tabletop thermoacoustic refrigerator for demonstrations. American Journal of Physics, 70(12), 1231–1233. https://doi.org/10.1119/1.1485720
12. Mahamuni1, P. Bhansali, P. Shah, N. and Parikh, Y. (2015).A Study of Thermoacoustic Refrigeration System. International Journal of Innovative Research in Advanced Engineering, vol. 2, no. 2, pp. 160–164
13. Ryan, T. S. (2010). Design and Control of a Standing-Wave Thermoacoustic Refrigerator. Retrieved from http://libproxy.txstate.edu/login?url=http://search.ebscohost.com/login.aspx?direct=true&db=edsndl&AN=edsndl.oai.union.ndltd.org.PITT.oai.PITTETD.etd-11132009-152225&site=eds-live&scope=site
14. Tijani, M., Zeegers, J., & de Waele, A. (2002). Design of thermoacoustic refrigerators. Cryogenics, 42(1), 49-57. doi: 10.1016/s0011-2275(01)00179-5.
15. D'Esposito, R., Balanethiram, S., Battaglia, J., Fregonese, S., & Zimmer, T. (2017). Thermal Penetration Depth Analysis and Impact of the BEOL Metals on the Thermal Impedance of SiGe HBTs. IEEE Electron Device Letters, 38(10), 1457-1460. doi: 10.1109/led.2017.2743043.

16. Zolpakar, N. A., Mohd-Ghazali, N., & Ahmad, R. (n.d.). Experimental investigations of the performance of a standing wave thermoacoustic refrigerator based on multi-objective genetic algorithm optimized parameters. APPLIED THERMAL ENGINEERING, 100, 296–303. https://doi.org/10.1016/j.applthermaleng.2016.02.028

17. Zolpakar, N. A., Mohd-Ghazali, N., Ahmad, R., & Maré, T. (2017). Performance of a 3D-printed Stack in a Standing Wave Thermoacoustic Refrigerator. Energy Procedia, 105, 1382–1387. https://doi.org/10.1016/j.egypro.2017.03.513.